



# Assessment of the Geochemical Potential in a Complex Tectonic Environment of South-East Sicily: New Insights From Hydrochemical Data

Gloria Maria Ristuccia<sup>1</sup>, Pietro Bonfanti<sup>1</sup>, Salvatore Giammanco<sup>1\*</sup> and Giuseppe Stella<sup>2</sup>

<sup>1</sup> Istituto Nazionale di Geofisica e Vulcanologia, Osservatorio Etneo, Sezione di Catania, Catania, Italy, <sup>2</sup> PH3DRA Laboratories (Physics for Dating Diagnostic Dosimetry Research and Applications), Dipartimento di Fisica e Astronomia, Università di Catania & INFN Sezione di Catania, Catania, Italy

## OPEN ACCESS

### Edited by:

Paolo Censi,  
University of Palermo, Italy

### Reviewed by:

Maria Aurora Armenta,  
National Autonomous University  
of Mexico, Mexico  
Jacob Clement Yde,  
Western Norway University of Applied  
Sciences, Norway

### \*Correspondence:

Salvatore Giammanco  
salvatore.giammanco@ingv.it  
ORCID: 0000-0003-2588-1441

### Specialty section:

This article was submitted to  
Geochemistry,  
a section of the journal  
Frontiers in Earth Science

**Received:** 01 February 2019

**Accepted:** 10 April 2019

**Published:** 26 April 2019

### Citation:

Ristuccia GM, Bonfanti P,  
Giammanco S and Stella G (2019)  
Assessment of the Geochemical  
Potential in a Complex Tectonic  
Environment of South-East Sicily:  
New Insights From Hydrochemical  
Data. *Front. Earth Sci.* 7:88.  
doi: 10.3389/feart.2019.00088

We analyzed a large dataset (143 water sampling sites, 22 variables) of chemical parameters in local groundwaters from the south-east sector of Sicily, namely the Hyblean plateau, in order to set an original evaluation of its geothermal potential using applied geochemistry. The area was affected by volcanism until about 1.4 Ma. Today, though no active volcanism occurs, it is site of surface gas manifestations of focused degassing to which a mantle source has been attributed. We identified and thence selected the most promising sites (water springs and wells) based both on their main geochemical characteristics and on their calculated equilibrium temperature (resulting in the range between 50 and 140°C). We then applied Principal Component Analysis (PCA) to this restricted dataset and we were able to discriminate between different sources of solutes, both natural and anthropogenic. Finally, we mapped the factor scores obtained from PCA and we focused on those likely related with geothermal conditions in order to highlight the areas with the highest geothermal potential.

**Keywords:** south-east Sicily, water geochemistry, geothermal energy, principal components analysis, geothermometry applications

## INTRODUCTION

Geothermics is a clean and sustainable source of energy, as geothermal power plants involve no combustion, unlike classic thermal power plants, and thus they emit very low levels of greenhouse gasses. Geothermal resources range from shallow ground reservoirs to vapor- or water-dominated systems accessed by drilling wells down to thousands of meters below the Earth's surface<sup>1,2</sup> (Bertani, 2012; Botteghi et al., 2012; Abate et al., 2014; Albanese et al., 2014). There is a growing interest in Italy on studies regarding the recognition of geothermal areas and their potential in terms of possible exploitation (Zervos et al., 2011).

However, still a large portion of the Italian territory has not been investigated, despite of clear evidence of existing geothermal systems (Minissale et al., 2019). Our study has been focused on a

<sup>1</sup><https://geothermal.org>

<sup>2</sup><http://geothermalweb.org>

south-eastern sector of Sicily, where volcanism has been active until middle Pleistocene and strong earthquakes have periodically occurred in historical times (Barberi et al., 1974; Dall'Aglio et al., 1995).

This sector of Sicily is today affected by several zones with focused gas emissions, diffuse degassing anomalies and thermal springs, in general associated with deep regional faults (Bonfanti et al., 1993; De Gregorio et al., 2002; Grassa, 2002; Grassa et al., 2006; Giammanco et al., 2007). The origin of the gases in the most intense emission points was found to be mantle (Bonfanti et al., 1993; Dall'Aglio et al., 1995; De Gregorio et al., 2002; Grassa, 2002; Giammanco et al., 2007).

The area under study is important also because: (i) it is densely populated (almost one million people live there, distributed among thirty-five municipalities); (ii) it is the site of two of the largest industrial centers of southern Italy; (iii) local land is used for many economic activities mostly related to agriculture (grapes, lemons, oranges, almonds, tomatoes, cheese, etc.). Exploitation of the local geothermal resources appears, therefore, of the utmost importance to provide both the population and the economic activities with a power source that is cheap, readily and widely available and with a low environmental impact, especially in a moment of world economic crisis mostly affecting the energy market.

Our purpose was to provide basic information in order to identify areas where there is a greater chance of finding viable geothermal conditions to be considered for future exploitation. Of all the many methodologies used to discover and characterize geothermal reservoirs (IGA Service GMBH, 2014), those based on geochemical surveys are among the most useful and reliable (D'Amore and Panichi, 1985; Nicholson, 1993).

This work is based on the evaluation and elaboration of already existing hydro-geochemical data collected by Istituto Nazionale di Geofisica e Vulcanologia – Palermo (INGV-PA) on behalf of the Regional Government of Sicily, that published the results on-line<sup>3</sup>. The present work is the first attempt to organize and elaborate this large set of data regarding the Hyblean area, in order to determine its geothermal potential, since only small specific areas have been studied in the past and only for the purpose of monitoring seismic activity (Bonfanti et al., 1993; Dall'Aglio et al., 1995).

## GEOLOGICAL AND HYDROLOGICAL SETTING

The Hyblean Mountains, with surface of about 4500 km<sup>2</sup>, occupy most of south-east Sicily and, from a geodynamic point of view, they belong to an important regional geological structure that includes the Hyblean-Malta Platform (Grasso and Lentini, 1982; Lentini et al., 1987) and that acts as junction between the Apennine-Maghrebic Chain in the northern part of the island and the northern boundary of the African plate. Three major active tectonic structures occur within the Hyblean Mts.: (i) the Gela Nappe along its north-west limit; (ii) a transcurrent faults

system crossing the whole central part of the area along a NNE-SSW direction and (iii) the Malta Escarpment located offshore along its east side, within the Ionian Sea (Adam et al., 2000).

The Hyblean foreland, along its northern and western edges, is bordered, instead, by a foredeep formed from a predominantly silico-plastic sedimentation derived from the northern areas during the Plio-Quaternary period (Labauve et al., 1990; Ristuccia et al., 2013). This sector was affected by the Plio-Quaternary tectogenesis that produced overlapping of the outer edge of the chain (Gela Nappe) over the most peripheral zone of the foreland.

This subsidence occurs with NE-SW faults systems on the northern edge, whereas its western margin is affected by a complex system interconnecting N-S- or NNE-SSW-directed tectonic lines (Scicli-F. Irminio Fault system) with NE-SE-trending faults (Ispica Fault on the SE of the study area and Comiso-Chiaramonte fault system on the W) (Figure 1).

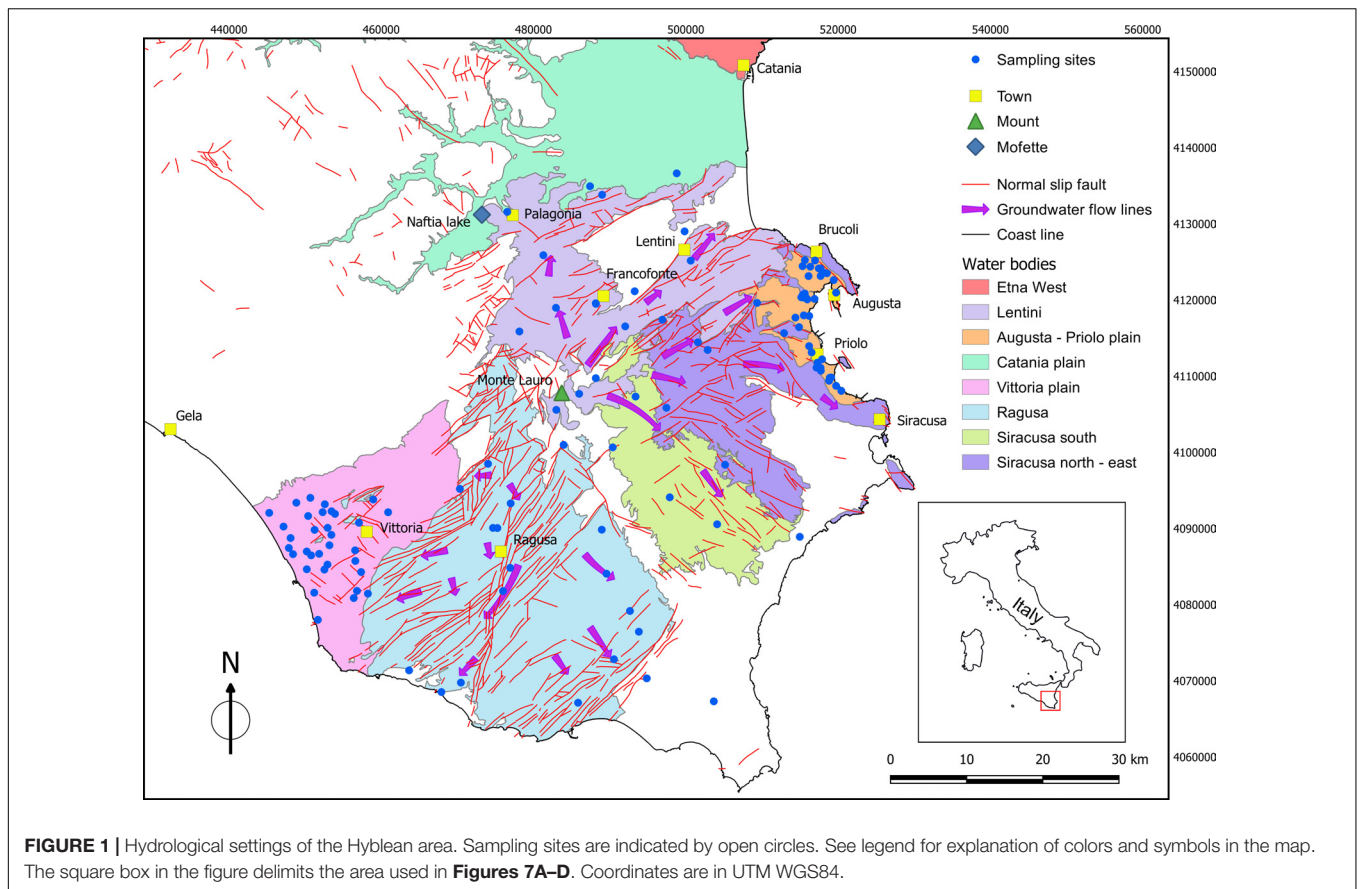
The Hyblean Mts. chiefly consist of a thick carbonate succession formed mainly as platform facies dated to Mesozoic-Cenozoic. The succession shows marked interbedding of volcanic deposits from several eruptive sequences that occurred in the area starting from the Cretaceous period (Bianchi et al., 1987). In particular, the northern margin of the Plateau was characterized by volcanism, both submarine and subaerial, until about 1.4 Ma (Schmincke et al., 1997). Subsequently, volcanic activity shifted toward the north, with eruptions occurring across the Catania Plain, and concentrated in the area where Mt. Etna would develop (Schiano et al., 2001).

The hydrogeological features of the Hyblean Plateau consist of carbonate rocks in its western part and of volcanic deposits in its eastern part. Both the volcanic and the carbonate aquifers above are characterized by high permeability, 10<sup>-5</sup> and >10<sup>-5</sup> m/s, respectively (Aureli et al., 1993). Due both to their high permeability and to their huge extension, these aquifers are the most important of south-east Sicily. In general, the area is often characterized by aquifers located at different depth, separated by horizontal layers of impermeable rocks, that, however, can be interconnected thanks to faults (Ruggieri, 1990). Piezometric contours in the study area indicate that groundwater flow occurs preferentially along radial directions, from the highest topographic areas (Monte Lauro) toward the low peripheral ones (Figure 1).

In general, local ground permeability is subject to marked decreases both vertically and laterally, because of fractures sealing and/or of contact with low-permeability marls. For these reasons, groundwater discharges occur along the entire length of the edge of the Hyblean Plateau (Ruggieri, 1990).

Coastal areas are bordered by sandy beaches crossed by limestone outcrops. The inter-tidal zone is characterized by many water springs that are usually the expression of discharge of groundwater that had infiltrated through limestone layers. Near shores, seawater shows a lower salinity than in the open sea because of the presence of groups of small freshwater springs. The Hyblean area can be divided into two main regions: a south-western sector, largely constituted by the Ragusa district and a north-eastern area, largely coinciding with the Siracusa territory and, in the least, with the Catania area.

<sup>3</sup>[http://www.regione.sicilia.it/presidenza/ucorirfuti/acque/pagina\\_1.htm](http://www.regione.sicilia.it/presidenza/ucorirfuti/acque/pagina_1.htm)



## South-West Sector

This sector is divided into two hydrogeological structures (water bodies): the Ragusa Basin and the Vittoria Plain Basin, respectively (**Figure 1**). In its west part (Comiso-Vittoria plain) two aquifers are present, the first being confined at moderate depth (from 50 to 100 m below the surface) within calcarenitic rocks and sandstone deposits of Pleistocene age, whereas the second is deeper and located in a carbonate substratum, confined by marls (Carbone et al., 1982, 1987; Grasso et al., 1982). The latter is a more productive aquifer and its depth varies according to the structural setting, being characterized by many blocks that were lowered or uplifted in a variable and irregular manner and that constitute the low part of the Hyblean plateau. Water supply in the western sector of the structural depression of Vittoria comes both from local infiltration of rain and from the carbonate massif. In this area there are some of the most important water springs in the whole plateau.

In the southwest sector of the study area the main outcropping rocks are limestones (Ragusa Formation) (**Figure 2**). These rocks host two different and superimposed aquifers, both with permeability due to fracturing, that in places are in hydraulic continuity due to the presence of important regional tectonic structures that cross them. The first aquifer is partly confined and it is located within calcarenitic sequence at an average depth between 100 and

150 m below the surface. The second aquifer, completely confined within marls and limestone, is larger than the previous one and it is separated from it by marly-clays with variable thickness.

Along the coastline and until their east boundary with the Siracusa territory, the limestone of the Ragusa Formation have an aquifer with discrete to good potential, confined by marls.

Lastly, alluvial deposits, depositional fans and recent sands in the Hyblean area generally host small aquifers with moderate to low productivity, due to their limited extension both horizontal and vertical.

## North-Eastern Sector

The northeast sector of the Hyblean plateau, from a hydrogeological point of view, can be subdivided into four water bodies: (i) Lentini basin; (ii) Siracusa north-east; (iii) Siracusa south; (iv) Augusta-Priolo plain. Those water bodies show different geochemical characteristics according to the directions of underground water flow. In particular, in the northern portion of the area investigated, from Monte Lauro to the Lentini plain, groundwater circulates predominantly into volcanic deposits of Pliocene-Pleistocene, with main flow directions toward north-east. The semi-permeable substratum of this aquifer is locally made of Miocene volcanic, whose upper layers are often weathered due to argillation processes. A structural high,

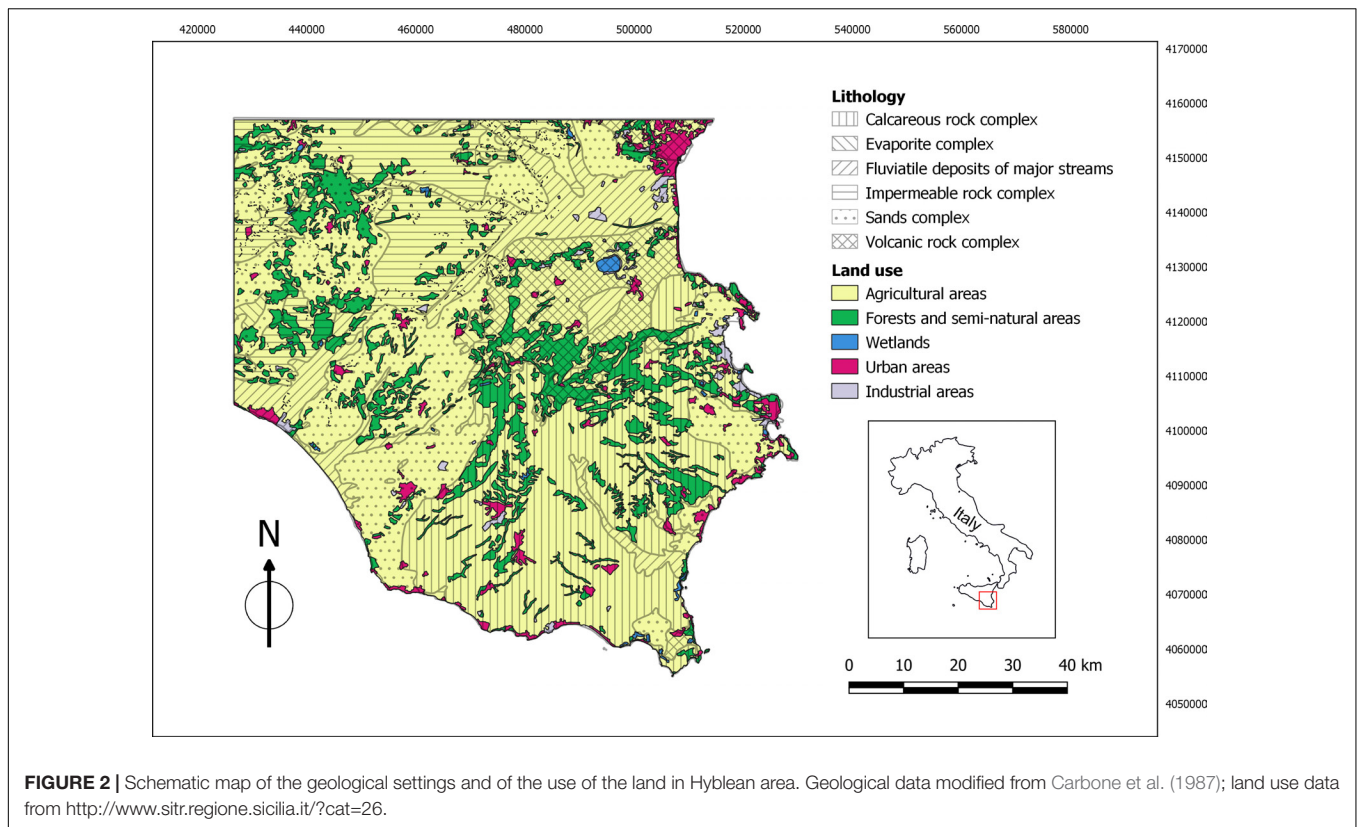


**FIGURE 2** | Schematic map of the geological settings and of the use of the land in Hyblean area. Geological data modified from Carbone et al. (1987); land use data from <http://www.sitr.regione.sicilia.it/?cat=26>.

directed NE-SO along on of the main tectonic lines in the region, separates this aquifer from the adjacent one of the Augusta-Priolo plain.

The latter shows a more marked alternation of deposits of volcanic origin and rocks belonging to the carbonate series. Further to the south is located the carbonate basin of Siracusa, delimited to the north by the Melilli-Monti Climiti graben, a structural high with WNW-ESE direction. In this basin groundwaters mostly flow toward the SW. The main aquifer in this basin occurs into limestone. The west part of this carbonate sequence rests on Miocene marls, whereas in the area of Siracusa and south of this town limestone are covered by more recent sediments of Pliocene-Pleistocene age. In general, this aquifer shows transmissivity values ranging from 0.1 to  $9 \times 10^{-3}$  m<sup>2</sup>/s and a relative high permeability due to karstification. The latter is a process that has affected the local Miocene carbonate series since its emersion.

The water body of the Augusta-Priolo plain is made of coarse sands and calcarenites, whose maximum thickness is scarcely greater than 20 m. Its substratum is composed of clays with variable thickness (from a few to some hundreds of meters). Where clays are missing, the sands and calcarenites rest directly on the lower permeable terms, with whom they are in hydraulic continuity.

Those rocks outcrop along the entire gulf of Augusta and inland up to a maximum altitude of 200 m. The water table existing within these rocks is exclusively fed from local infiltration and it is largely drained by the local water streams.

## MATERIALS AND METHODS

Geochemical methods have a relatively low cost and provide precious information both on the source(s) of water and, in the case of a geothermal system, on the temperature conditions of the fluids in the reservoir.

In particular, the use of geochemical surveying in geothermal exploration is of great importance for the inference of subsurface thermal conditions through chemical analysis of fluids discharged at the surface (Dolgorjav, 2009).

Between 2004 and 2005, one hundred and thirty seven waters samples from springs and wells throughout basins of the southeastern Sicily were collected and immediately analyzed in the laboratories of INGV-PA. Details on field and laboratory procedures are available at [http://www.regione.sicilia.it/presidenza/ucomrifuti/acque/pagina\\_1.htm](http://www.regione.sicilia.it/presidenza/ucomrifuti/acque/pagina_1.htm).

The determination of the water temperature, electrical conductivity, TDS and  $\text{HCO}_3^-$  was carried out directly in the field. Unfortunately, water pH was not measured. The concentration of  $\text{HCO}_3^-$  was determined by titration with HCl 0.1 N. Chemical analyses of major ions were performed by ion-chromatography (Dionex DX 120) on filtered (0.45  $\mu\text{m}$  Acrodisc® cellulose filters) and acidified (100  $\mu\text{m}$   $\text{HNO}_3$  SUPRAPUR®) samples, with reproducibility within  $\pm 2\%$ . A Dionex CS-12A column was used for the determination of major cations ( $\text{Na}^+$ ,  $\text{K}^+$ ,  $\text{Mg}^{2+}$ ,  $\text{Ca}^{2+}$ ) and a Dionex AS4A-SC column was used for the major



anions ( $F^-$ ,  $Cl^-$ ,  $NO_3^-$ ,  $SO_4^{2-}$ ) (Sortino et al., 1991). Trace element analyses were performed by a Perkin Elmer ELAN-DRC-e ICP-MS. Accuracy and precision (<5%) of the measures were computed by analyzing certified reference materials and by performing several replicates on samples. The detection limits for all analyzed elements was in the range 0.01–0.1  $\mu\text{g/l}$ .

Some of the sites were sampled in both years. We observed that the analytical results for duplicate samples were very similar in time, so we decided to consider only the 2005 samples.

Furthermore, in order to improve the statistical results, another six waters samples extracted from Dall'Aglio et al. (1995) were considered and added to our database. The analytical methods for these six samples are reported in Dall'Aglio et al. (1995).

In all cases, the accuracy of major element analyses was checked by using charge mass balances. Analyses were considered as acceptable when the charge imbalance was less than 10%. The only exceptions were samples Vanghella-Palagonia and the samples from Dall'Aglio et al. (1995). In the first case the imbalance excess was very small (−11.04%), whereas in the latter samples imbalances were attributed to the lack of data on nitrates. In all cases, the overall meaning of the analyses was believed not to be affected in a substantial way.

## RESULTS AND DISCUSSION

### Geochemical Classification of Analyzed Waters

The chemical data analyzed in this paper are shown in **Appendix 1 of Supplementary Material**.

In the tables of this **Appendix**, we distinguished between the 111 sites sampled in 2005 and the six sites described by Dall'Aglio et al. (1995). **Appendix 2 of Supplementary Material** shows some basic statistics (mean, minimum value, maximum value, standard deviation, median) on the available parameters, divided by basins.

According to the Langelier-Ludwig diagram (Langelier and Ludwig, 1942), where the relative concentrations of major constituents are considered, the sampled waters show a wide range in chemical composition (**Figure 3**), with the majority of the sites displaying a bicarbonate alkaline-earth composition, which is typical of the majority of the groundwaters flowing into shallow aquifers. Another large group of samples shows a composition highly enriched in  $SO_4^{2-}$  and secondarily in  $Ca^{2+}$ . These sites belong to the same basin, located near the town of Vittoria, where most of the land is extensively cultivated with grapes. It is therefore possible that their peculiar composition reflects pollution by wastewaters rich in  $NH_4$ , Ca, and  $SO_4$  caused by local agricultural activities (Aiuppa et al., 2002, 2003). Finally, a third important group of waters shows a composition trending toward an alkali-Cl composition, from an initial alkaline-earth composition. These waters are seemingly divided into two sub-groups: (i) one shows a compositional trend toward seawater and it is

actually made of samples generally from sites close to the coast lines and hence most subject to seawater intrusion; (ii) another group seems to result from mixing between the typical composition of shallow groundwaters and geothermal brines and therefore will be analyzed in greater detail in the following section of this work.

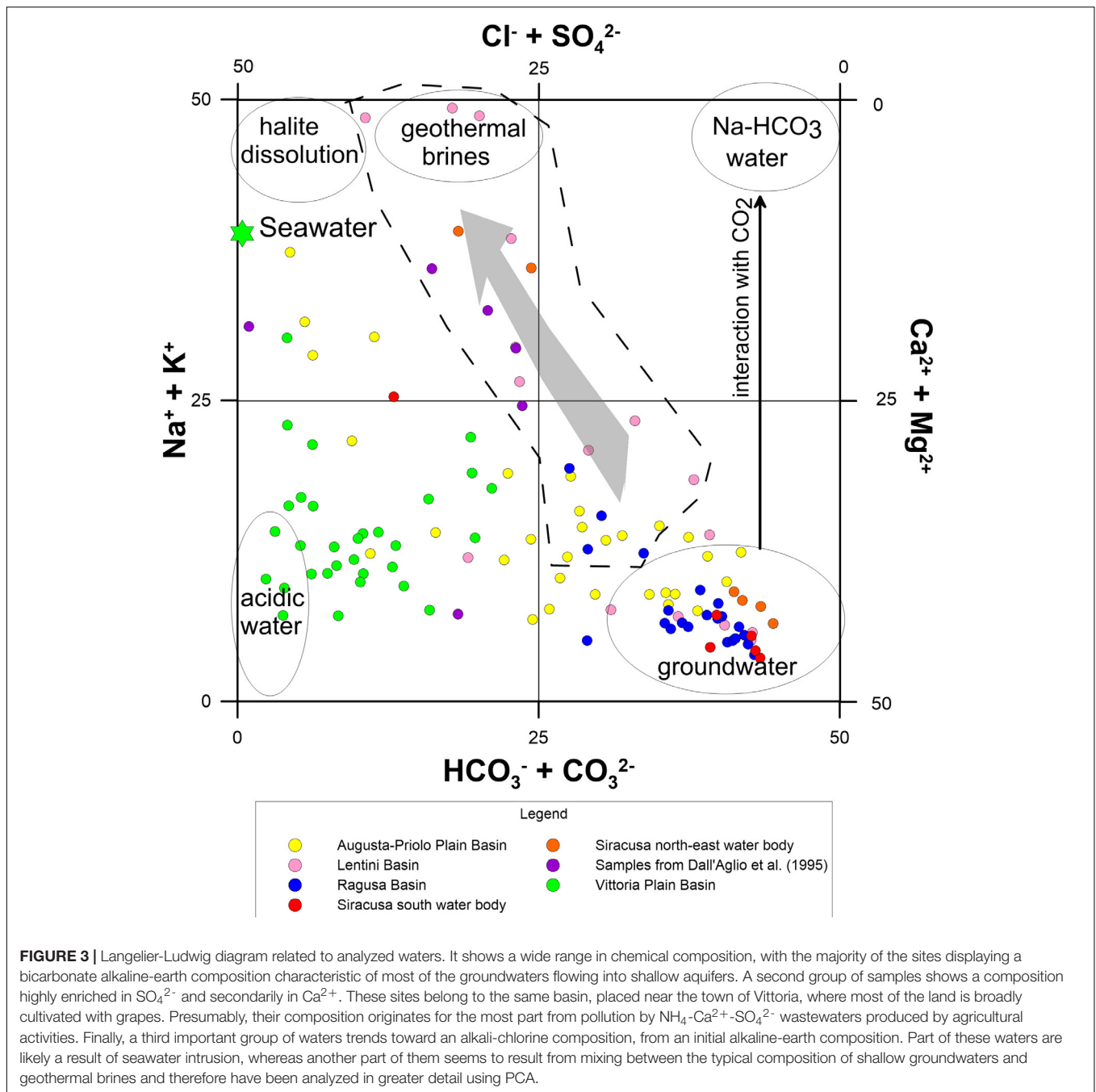
The  $HCO_3$ - $SO_4$ -Cl ternary diagram (**Figure 4**) better highlights what already suggested by the Langelier-Ludwig diagram. We show here the modified version of this triangular diagram, according to Giggenbach (1988), in order to classify geothermal fluids based on their major anions concentration. The modified graph helps to discern between mature geothermal fluids and immature and unstable waters. It also gives preliminary indication of mixing processes and/or geographic clustering. The graph shows clearly that (i) most of the samples fall close to the  $HCO_3$  corner, typical of shallow groundwater; (ii) all of the samples from the Vittoria basin are highly enriched in  $SO_4^{2-}$ , most probably because of strong water pollution due to agricultural activities related to wine production (with often massive use of sulfide-bearing fertilizers and fungicides); (iii) several samples trend toward the composition typical of mature geothermal waters. The latter mostly correspond to the samples indicated by the Langelier-Ludwig diagram for the waters mixing with geothermal brines. An exception in this group is a sample from the Lentini Basin (Bevaio Basso\_Buccheri in **Appendix 1**), whose composition from the Langelier-Ludwig diagram falls almost at the extreme of the chlorine alkaline-earth quadrant, being also close to the “acidic water” field.

### Aqueous Geothermometers

Application of chemical geothermometers to groundwaters is one of the main methods in the exploration of geothermal resources. It allows to foresee subsurface water temperatures and to get precious information about the evolution of a geothermal reservoir during exploitation. Geothermometry is based on the assumption that water attains a temperature-dependent equilibrium with the minerals in the host rock of the reservoir. However, water in geothermal reservoirs generally shows temperature values that are not homogeneous and temperature gradients may occur both horizontally and vertically. For this reason, the temperatures measured in deep drill-holes may be higher than those inferred from chemical geothermometry, particularly in the case of waters that come from shallow aquifers (Arnórsson et al., 1983). In any case, the use of water geothermometers is fundamental to get at least an idea of the minimum temperature that can be encountered in a given reservoir.

Based on the previous geochemical characterization of the sampled waters, we selected thirty-three sites of the initial group, considering only those whose chemical compositions in the Langelier-Ludwig and  $HCO_3$ - $SO_4$ -Cl ternary diagrams (**Figures 3, 4**) fall close to that of geothermal waters or show an evident mixing line toward geothermal waters. These samples are also highlighted in **Appendix 1 of Supplementary Material**.

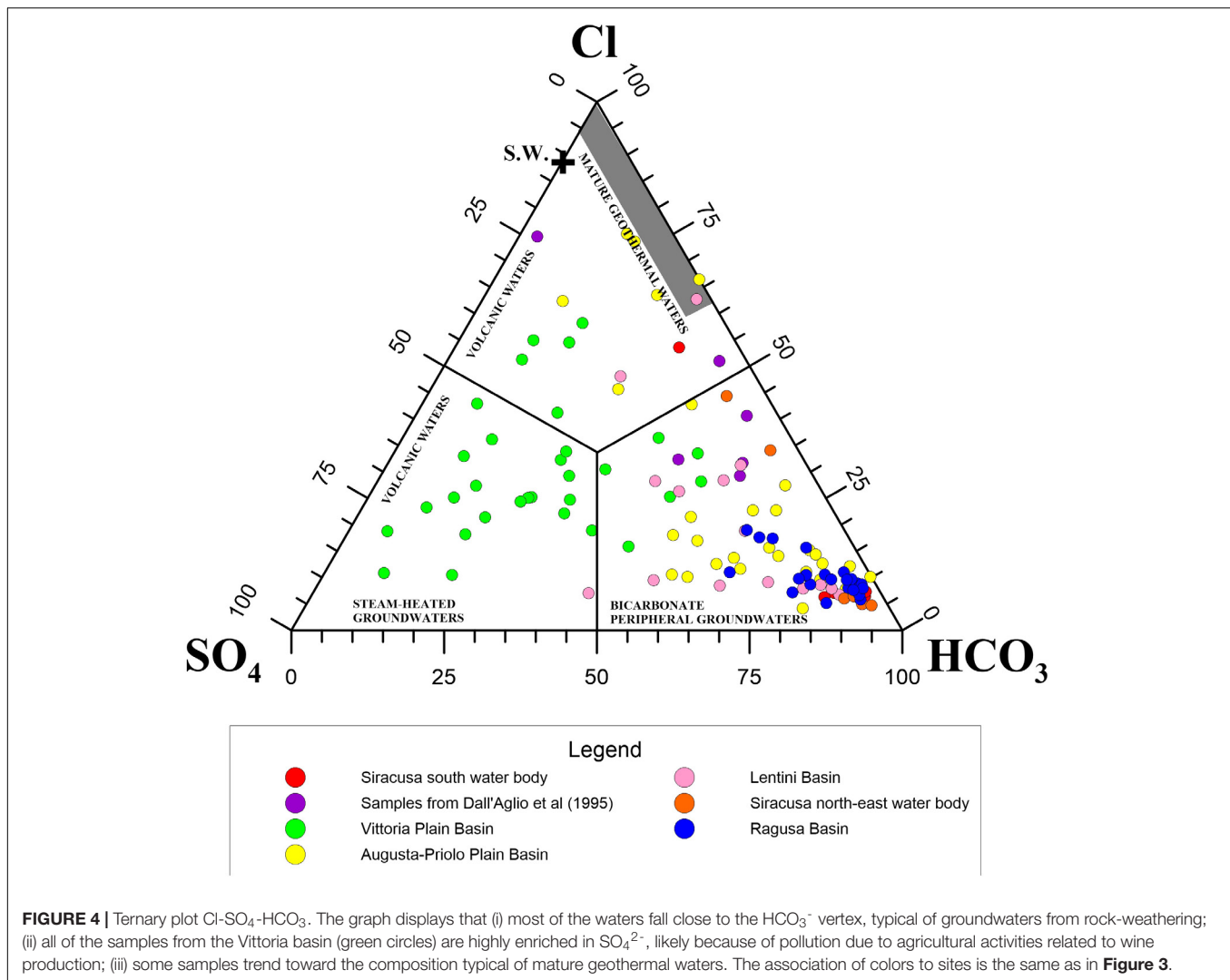
The  $K^2/Mg$  and  $K^2/Ca$  (Fournier and Truesdell, 1973) geothermometers are among the most important. By combining



the two geothermometers above, Giggenbach (1988) obtained a very useful graphic method for assessing the degree of attainment of water-rock equilibrium. **Figure 5** shows the triangular plot of Giggenbach (1988) for the selected water samples. Most of the samples fall close to the  $\text{Mg}^{1/2}$  corner, thus being far from equilibrium and indicating a low water temperature at depth. However, three samples – namely Paparone\_Virgonello, Tenuta Rannè\_Lentini and Rendo\_Catania – fall within the partially equilibrated waters field, along curves toward the  $\text{Mg}^{1/2}$  vertex that suggest equilibration temperature ranging between about 100 and 140°C. This is interpreted as cooling of thermal water

upon migration toward the surface and its Mg enrichment during water-rock interaction.

Furthermore, we plotted the analytical results of the thirty-three selected sites in a graph of  $\log(\text{K}^2/\text{Mg})$  vs.  $\log(\text{K}^2/\text{Ca})$ , which is another graph frequently used to evaluate both the temperature of final water-rock equilibrium and the  $\text{PCO}_2$  of geothermal liquids (**Figure 6**). As for the triangular plot of **Figure 5**, most of the samples fall out of the temperature range of geothermal interest, also in this case showing “immature” conditions. Several samples, however, fall well within the conditions of geothermal interest, indicating



temperature values in the range between about 50°C and about 90°C.

Some data points plot below the “calcite formation” line and most of them have PCO<sub>2</sub> values higher than those at full equilibrium. These conditions favor conversion of Ca-Al-silicates to calcite in the sampled waters, whose chemistry is seemingly controlled by dissolution of the host rock rather than by equilibrium between water and minerals.

The highest PCO<sub>2</sub> values indicated in this plot (samples labeled A–F) are in the same range as those calculated in the groundwaters of Mt. Etna volcano, where the origin of dissolved CO<sub>2</sub> is mostly from magma degassing at depth and where high PCO<sub>2</sub> values are found associated with slight thermal anomalies in water (Allard et al., 1997; Giammanco et al., 1998; Brusca et al., 2001; Aiuppa et al., 2002, 2003). The association observed in **Figure 6** between high values of calculated dissolved CO<sub>2</sub> and high values of calculated temperature in our samples, therefore, suggests a possible origin of CO<sub>2</sub> from mantle degassing also for these waters. It is worth of note that huge emissions of CO<sub>2</sub> and helium from a mantle source occur from a site – namely, Naftia

Lake – located near the town of Palagonia, at the NW limit of the studied area (**Figure 1**) and close to the sites of the above water samples (De Gregorio et al., 2002; Giammanco et al., 2007).

## Principal Component Analysis

We used a particular type of multivariate statistical analysis – namely Principal Component Analysis (PCA) – in order to distinguish between the different possible sources of solutes in our sampled waters. All calculations were performed using the STATISTICA™ software. In our case, only the factors with eigenvalue greater than one were considered in the development of the analysis. The matrix of orthogonal factors thus calculated was then rotated using the Normalized Varimax procedure. The coefficients that quantify the relative weight of single factors in the linear combination are called loadings. Six independent factors were extracted (**Table 1**) and they explain 85.3% of the total variance (**Table 2**). Factor one is responsible for 39.4% of the overall variance and shows water T° and K negatively correlated with water hardness, Ca<sup>2+</sup>, NO<sub>3</sub><sup>-</sup>, Ba, Hg, and Se. Factor two is responsible for 13.9% of the overall variance and

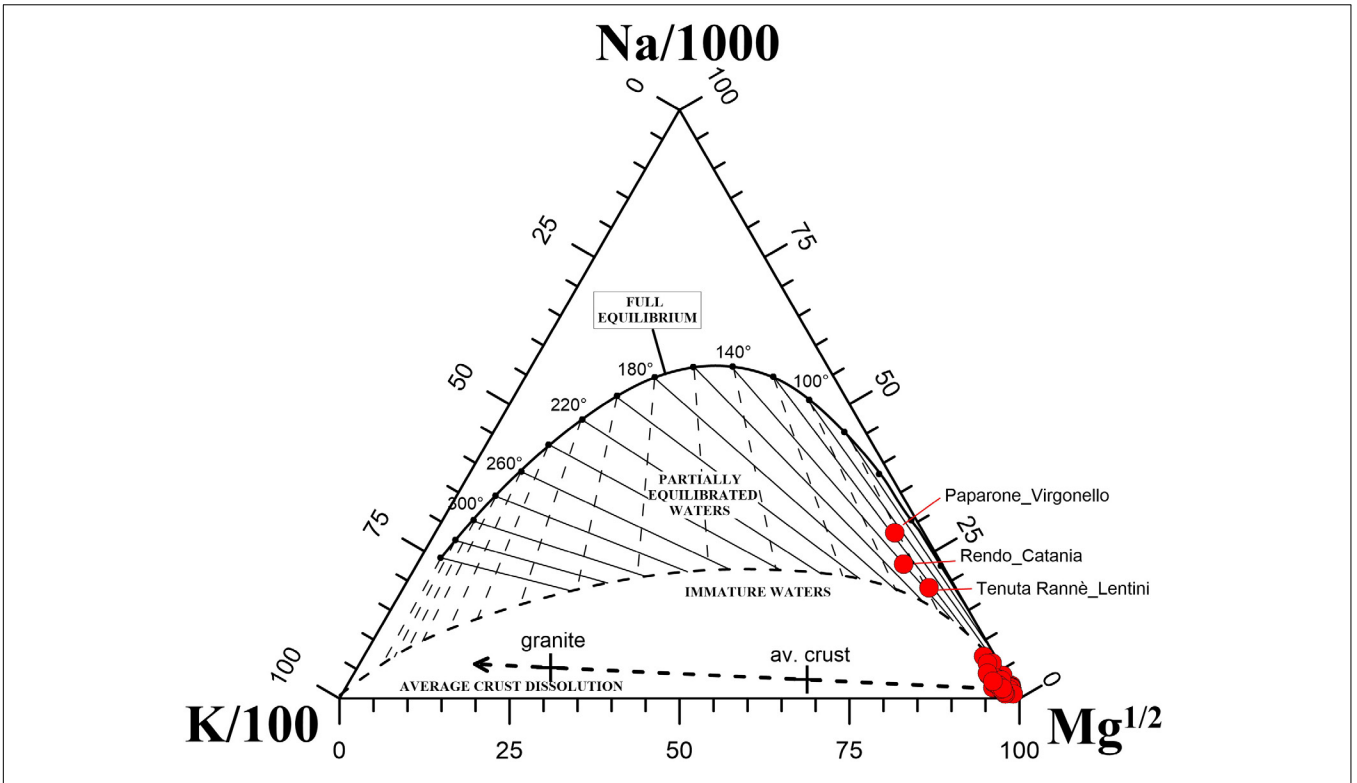


**FIGURE 5** | K-Mg-Na ternary diagram (modified from Giggenbach, 1988) for the 33 selected water samples in the area investigated. Samples showing conditions of partial equilibration are indicated with their name.

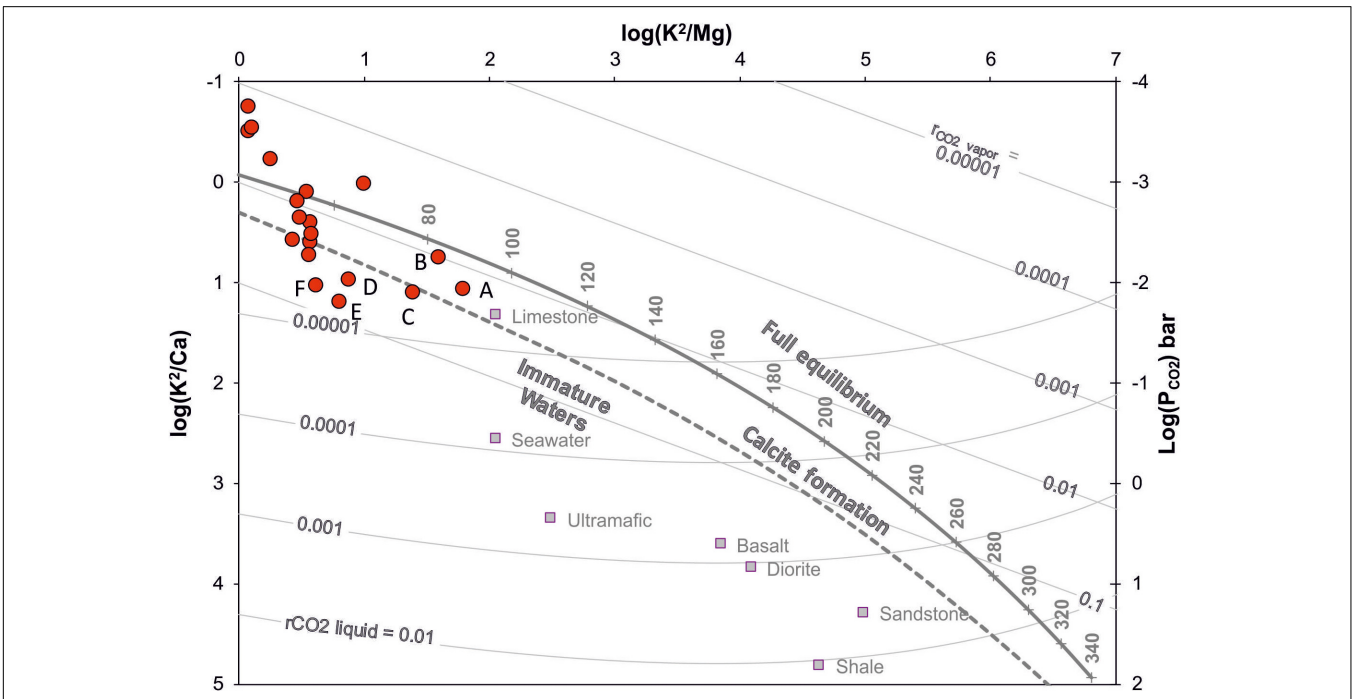


**FIGURE 6** | Graph of  $\log(K^2/Mg)$  vs.  $\log(K^2/Ca)$  for some selected sites (see text for explanation). Some waters fall well within the conditions of geothermal interest, showing calculated equilibrium temperature values in the range between about 50°C and about 90°C.



is represented by hardness, conductivity,  $\text{Na}^+$ ,  $\text{K}^+$ ,  $\text{Mg}^{2+}$ ,  $\text{Cl}^-$ , Cu, Hg, and Se. The third factor is responsible for 11.5% of the overall variance and includes  $\text{SO}_4^{2-}$ , B, Cu, and  $\text{F}^-$ . The fourth factor is responsible for 10.6% of total variance, and includes hardness,  $\text{Ca}^{2+}$ ,  $\text{Mg}^{2+}$ ,  $\text{HCO}_3^-$ , Ba, Cu,  $\text{F}^-$ , Fe, Mn, Se, and As. The fifth factor is responsible for 5.4% of overall variance, showing  $\text{SO}_4^{2-}$  negatively correlated with Pb. Finally, the sixth factor is responsible for 4.6% of overall variance; it is represented only by Zn.

The first factor would be indicative of water pollution from human sources, likely due to agricultural activity because of the high loadings of  $\text{NO}_3^-$  and Hg. In particular, the highest levels of  $\text{NO}_3^-$  are found in the SW part of the study area (**Appendix 1 of Supplementary Material**), where fertilizers are widely used in the local agricultural activities focused on wine production (this area is actually that with the largest vineyards in all east Sicily). Furthermore, the highest Hg concentrations (**Appendix 1 of Supplementary Material**) occur near the town of Priolo (NE part of the study area), near one of the largest oil refineries of Sicily. The second factor seems to be the expression of hydrothermal conditions in the studied aquifers. In fact, many of the parameters showing the highest loadings (in particular  $\text{K}^+$ ,  $\text{Cl}^-$ , Cu, and Se) are proxies of such conditions. The third factor is also likely related with hydrothermal conditions in the studied groundwaters. In particular, in this factor a high sulfate loading would indicate oxidation of hydrothermal  $\text{H}_2\text{S}$ , although the possibility of some sulfate input from agricultural activities cannot be ruled out, especially

in the SW part of the study area for the same reasons given for factor 1.

Factor 4 is likely expression of dissolution of Ca- and Mg-bearing carbonate rocks. However, it could also be an indication of input of magmatic gasses directly into “cold” aquifers, with consequent strong water-gas-rock interaction highlighted by the high loading of  $\text{HCO}_3^-$ . The last two factors account for very low values of the total variance; besides, they are best represented by only one parameter, so they will not be considered in our later discussion for the aims of our study.

## Mapping of Factors

In order to better constrain the geochemical processes revealed by PCA, we performed surface mapping with Surfer® and using the Kriging method (Swan and Sandilands, 1995), analyzing the factor scores of the first four factors extracted from the multivariate analysis (**Table 3**). The maps thus produced (**Figures 7A–D**) helped us in the evaluation of the spatial distribution of the extracted factors.

**TABLE 2** | Parameters from PCA for the main four factors extracted.

Factor	Eigenvalue	% Total variance	Cumulative Eigenvalue	Cumulative %
1	3.056	13.890	11.718	53.264
2	2.528	11.490	14.246	64.754
3	2.327	10.579	16.573	75.333
4	1.189	5.405	17.762	80.739

**TABLE 1** | Factors extracted from the PCA for the parameters analyzed.

	Factor 1	Factor 2	Factor 3	Factor 4	Factor 5	Factor 6
T (°C)	<b>-0.761</b>	0.070	0.074	-0.385	0.189	0.003
Hardness (mg/l)	<b>0.725</b>	<b>0.445</b>	0.026	<b>0.477</b>	0.068	-0.067
Conductivity ( $\mu\text{S}/\text{cm}$ )	0.282	<b>0.896</b>	0.138	0.249	0.066	0.040
$\text{Na}^+$ (mg/l)	-0.001	<b>0.904</b>	0.301	0.115	0.036	0.069
$\text{K}^+$ (mg/l)	<b>-0.505</b>	<b>0.767</b>	-0.122	0.027	-0.233	0.016
$\text{Ca}^{2+}$ (mg/l)	<b>0.834</b>	0.264	-0.003	<b>0.402</b>	0.129	-0.070
$\text{Mg}^{2+}$ (mg/l)	-0.059	<b>0.816</b>	-0.274	<b>0.414</b>	-0.055	-0.006
$\text{Cl}^-$ (mg/l)	0.284	<b>0.910</b>	0.111	0.207	0.050	0.055
$\text{SO}_4^{2-}$ (mg/l)	0.039	0.025	<b>0.789</b>	-0.219	<b>0.430</b>	-0.057
$\text{HCO}_3^-$ (mg/l)	0.020	0.253	0.163	<b>0.740</b>	-0.150	-0.147
$\text{NO}_3^-$ (mg/l)	<b>0.627</b>	-0.116	-0.004	-0.202	-0.007	-0.038
B ( $\mu\text{g}/\text{l}$ )	-0.105	0.091	<b>0.890</b>	0.123	-0.280	-0.042
Ba ( $\mu\text{g}/\text{l}$ )	<b>0.464</b>	0.051	0.014	<b>0.758</b>	0.078	-0.244
Cu ( $\mu\text{g}/\text{l}$ )	0.313	<b>0.410</b>	<b>0.600</b>	<b>0.513</b>	-0.080	0.072
$\text{F}^-$ ( $\mu\text{g}/\text{l}$ )	0.124	0.049	<b>0.776</b>	<b>0.414</b>	-0.302	0.127
$\text{Fe}_{\text{tot}}$ ( $\mu\text{g}/\text{l}$ )	0.017	0.289	0.083	<b>0.879</b>	0.048	0.013
Mn ( $\mu\text{g}/\text{l}$ )	0.060	0.012	-0.004	<b>0.817</b>	0.082	0.115
Pb ( $\mu\text{g}/\text{l}$ )	-0.008	-0.005	0.160	-0.100	<b>-0.871</b>	0.032
Zn ( $\mu\text{g}/\text{l}$ )	0.102	-0.108	-0.010	-0.006	0.039	<b>-0.964</b>
Hg ( $\mu\text{g}/\text{l}$ )	<b>0.665</b>	<b>0.441</b>	0.286	-0.148	0.059	-0.029
Se ( $\mu\text{g}/\text{l}$ )	<b>0.465</b>	<b>0.592</b>	0.291	<b>0.505</b>	0.089	0.141
As ( $\mu\text{g}/\text{l}$ )	0.030	0.284	0.091	<b>0.867</b>	0.016	0.114

Significant values ( $> \pm 0.4$ ) are highlighted in bold.

**TABLE 3** | Factor scores extracted from the multivariate analysis (PCA) relative to the selected group of thirty-three sites (see **Appendix 1** for explanation of cases).

Case	Factor 1	Factor 2	Factor 3	Factor 4
1	0.591	-0.817	0.569	0.106
2	1.537	-0.010	-0.414	-0.191
3	1.998	3.351	0.728	-1.365
4	0.592	-0.630	-0.251	-0.315
5	0.603	-0.738	-0.537	-0.214
6	0.592	-0.559	-0.424	-0.026
7	0.688	-0.908	0.031	0.374
8	1.508	1.853	0.155	-0.701
9	-0.332	2.778	-0.381	3.453
10	0.285	-1.322	-0.452	1.577
11	0.525	-0.505	1.016	3.289
12	0.628	-0.777	-0.088	0.260
13	2.245	-0.831	0.006	-0.735
14	-0.391	-0.168	0.082	0.493
15	0.884	-0.665	0.132	0.175
16	0.203	-0.581	-0.872	0.216
17	0.172	-0.279	0.034	0.043
18	-0.555	-0.064	-0.206	-0.286
19	-1.127	-0.277	4.306	-0.092
20	-1.339	-0.329	0.390	-0.551
21	-0.186	-0.502	-0.824	-0.475
22	-0.469	-0.240	0.420	-0.449
23	-0.861	0.341	1.626	-0.780
24	-0.208	-0.227	-0.621	-0.510
25	-0.594	-0.297	-0.337	-0.577
26	-1.081	-0.067	0.271	-0.684
27	-0.298	0.232	0.754	-0.466
28	-0.682	0.097	-0.413	-0.334
29	0.603	-0.167	-0.497	-0.368
30	-1.382	0.311	-0.917	-0.228
31	-1.256	0.268	-1.004	-0.198
32	-1.620	1.165	-1.119	-0.298
33	-1.273	0.563	-1.162	-0.144

The map of Factor 1 (**Figure 7A**) was obtained with a standardized variogram and a linear fitting model (Nugget of 0.3; Range of 29,000; Sill of 2.22). In this study, it was the only case of a model produced with a linear best fitting, likely due to the erratic nature of the random function that describes the factor analyzed, which in turn produces an infinite variance of the process under consideration. Actually, this factor includes variables linked to human pollution from agricultural activities, a rather ubiquitous process in the study area. The map shows the presence of high values in the SW and SE parts of the study area. In particular, the maximum values of this factor are observed near the town of Priolo, located just north of Siracusa. As above mentioned, this area is known for the presence of one of the three oil refineries of Sicily and the only one in east Sicily (the other two being located near Milazzo on the northern coast of the island and near Gela on the southern coast), which might explain the pollution from elements connected with such industrial activity (e.g., Hg).

Other high values of this factor are located around the town of Ragusa, in an area with intensive cultivation of grapes and thence exposed to heavy pollution from fertilizers, as above described.

The map of Factor 2 (**Figure 7B**) was obtained with a standardized variogram and a spherical fitting model (Nugget of 0.5; Range of 29,000; Sill of 3.21). The maximum values of this factor are located, again, close to Priolo and in the NE corner of the investigated area. Although being near the oil refinery area of Priolo, the sites with the highest scores of this factor are mostly located north of it, closer to an already known area with marked signs of presence of hydrothermal fluids (Dall'Aglio et al., 1995), best evidenced by a sulphureous hot water spring near the village of Brucoli (Highlighted in **Figure 1**). It is an area crossed by several deep tectonic faults, some of which are potentially seismogenic (Basili et al., 2008), likely acting as pathways for the rise of high-enthalpy deep fluids. The zone further to the north of this area is also known for the presence of warm water wells, several zones with high diffuse degassing of carbon dioxide and some mofettes with focused emission of mantle gasses, the most important of which is the Naftia Lake (**Figure 1**) (Bonfanti et al., 1993; De Gregorio et al., 2002; Giammanco et al., 2007).

It is worth of note that this area, near the town of Palagonia, was site of volcanic activity during recent geological periods, until Pleistocene (Barberi et al., 1974; Behncke, 2004) and it is crossed, too, by important tectonic faults.

The map of Factor 3 (**Figure 7C**) was also obtained with a standardized variogram and a spherical fitting model (Nugget of 0.5; Range of 29,000; Sill of 4.71). The spatial distribution of this factor clearly shows a nice correspondence between its highest values and the zones closest to the already known areas with circulation of hydrothermal fluids (Bonfanti et al., 1993; Dall'Aglio et al., 1995; De Gregorio et al., 2002; Giammanco et al., 2007), thus confirming the interpretation given to this factor and making this factor the most important and reliable for the assessment of potential geothermal resources.

The map of Factor 4 (**Figure 7D**) was again obtained with a standardized variogram and a spherical fitting model (Nugget of 0.4; Range of 29,000; Sill of 5.93). Two main areas with high values can be observed in this map, corresponding to the sectors with the highest concentration of tectonic faults. Similar to the distribution of factor 2 scores, the maximum values are located, once more, north of Priolo and close to the sulphureous spring near Brucoli. This points to the attribution of factor 4 mainly to input of deep CO<sub>2</sub> to the aquifer, rather than to limestone dissolution only, thus marking the important role of the active tectonic faults in the area as pathways for the upward migration of deep magmatic fluids. Presence of high-pressure deep fluids (chiefly CO<sub>2</sub> gas) along fault planes is crucial in triggering fault motion and potential earthquake rupture by reducing fault strength (Rice, 1992; Sibson, 1992, 2000; Cox, 1995; Chiodini et al., 2004). This strengthens the hypothesis that these faults are at least in part responsible for the generation of earthquakes in this part of Sicily (Amato et al., 1995). The second zone with high values of this factor seems also spatially related with the most important regional fault lines in SE Sicily, as above

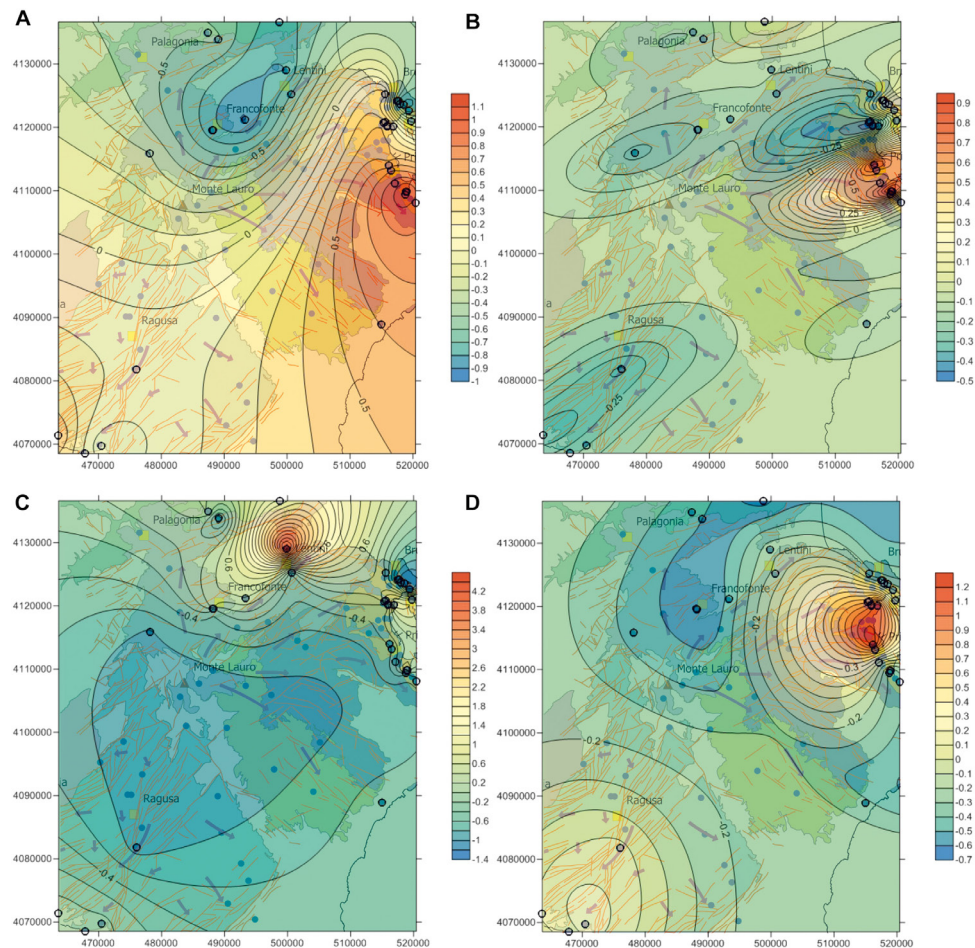


**FIGURE 7** | Maps of the spatial distribution of the scores of first four factors extracted from the PCA. **(A)** factor 1, indicative of water pollution from human factors; **(B)** factor 2, indicative of hydrothermal conditions in the studied aquifers; **(C)** factor 3, likely related with hydrothermal conditions in the studied groundwaters; **(D)** factor 4, that indicates areas affected by release of magmatic gasses with almost no heat carried by them. The base maps are extrapolated from the map in **Figure 1**.

cited (Sciqli-F. Irminio Fault system, trending N-S or NNE-SSW, and the Comiso-Chiaramonte fault system, trending NE-SE). In this case, the parameters belonging to this factor would suggest rise of magmatic gasses with almost no heat carried by them. The source of gas would be the mantle itself, as suggested by isotopic values of He and C of  $\text{CO}_2$  measured in local dissolved gasses (Grassa, 2002; Grassa et al., 2006).

## CONCLUSION

This study represents the first attempt to use a large dataset of chemical parameters in groundwaters from the Hyblean area in SE Sicily for the assessment of the local geothermal potential.

Using the appropriate classification diagrams, it was possible to highlight the sites whose water chemistry is the closest to that typical of geothermal environments.

By applying the PCA to the data from those sites, we were able to further investigate the causes for the observed chemical features of groundwater. Among the different sources

of dissolved chemicals, often acting together at a same site, some were related to pollution from local human activities (mostly related with agriculture, as it is the main land use in the region, see **Figure 2**), some to possible input of deep magmatic fluids (likely rising from the mantle through active regional faults, as suggested from the presence of sites with strong emission of mantle-derived  $\text{CO}_2$  in the area), some others to circulation of geothermal fluids. Mapping of the factor scores for the “geothermal source” revealed from PCA allowed us to discriminate the areas with the highest geothermal potential.

The results indicated clearly that the study area – affected by volcanism until the middle Pleistocene – is still site of active mantle degassing, providing an almost inexhaustible source of heat to the existing geothermal reservoirs.

This work is primarily intended to serve as a basis for future works in the same area that will use new data, more specifically focused on those parameters linked to geothermal conditions. The final purpose is to prepare the ground for a future exploitation of the area. The analyses presented here will also implement the knowledge on how to use hydro-geochemistry for



the assessment of the geothermal potential in low-temperature systems, similar to what has already been done in other areas of the world (e.g., Sanliyuksel and Baba, 2011; Asta et al., 2012; Blasco et al., 2018; Morales-Arredondo et al., 2018).

The preliminary analysis presented here looks promising in view of a future extensive use of the geothermal resource. Given the widespread use of the land for agricultural and farming purposes (the area is famous for the production of wine, tomatoes and vegetables in general, oranges and other fruits, cheese, as well as for cattle and fish farming) and the large urbanization in SE Sicily, exploitation of low-enthalpy geothermal systems such as those described in this work appears as a major resource for the support and promotion of economic development in the region.

## REFERENCES

- Abate, S., Botteghi, S., Caiozzi, F., Desiderio, G., Di Bella, G., Donato, A., et al. (2014). *VIGOR: Applicazioni Geotermiche Per uno Sviluppo sostenibile. Produzione di Calore ed Energia Elettrica. In Progetto VIGOR - Valutazione del Potenziale Geotermico delle Regioni della Convergenza, POI Energie Rinnovabili e Risparmio Energetico 2007-2013*. Pisa: CNR-IGG.
- Adam, J., Reuther, C. D., Grasso, M., and Torelli, L. (2000). Active fault kinematics and crustal stresses along the Ionian margin of southeastern Sicily. *Tectonophysics* 326, 217–239. doi: 10.1016/S0040-1951(00)00141-4
- Aiuppa, A., Bellomo, S., Brusca, L., D'Alessandro, W., and Federico, C. (2003). Natural and anthropogenic factors affecting groundwater quality of an active volcano (Mt. Etna, Italy). *Appl. Geochem.* 18, 863–882. doi: 10.1016/S0883-2927(02)00182-8
- Aiuppa, A., Brusca, L., D'Alessandro, W., Giammanco, S., and Parello, F. (2002). "A case study of gas-water-rock interaction in a volcanic aquifer: the south-western flank of Mt. Etna (Sicily)," in *Water-Rock Interaction*, eds I. Stober and K. Bucher (Netherlands: Kluwer Academic Publishers), 125–145. doi: 10.1007/978-94-010-0438-1\_5
- Albanese, C., Allansdottir, A., Amato, L., Ardizzone, F., Bellani, S., Bertini, G., et al. (2014). *VIGOR: Sviluppo Geotermico Nelle Regioni Della Convergenza. In Progetto VIGOR - Valutazione del Potenziale Geotermico delle Regioni della Convergenza. POI Energie Rinnovabili e Risparmio Energetico 2007-2013*. Pisa: CNR - IGG. doi: 10.1007/978-94-010-0438-1\_5
- Allard, A., Jean-Baptiste, P., D'Alessandro, W., Parello, F., Parisi, B., and Flehoc, C. (1997). Mantle-derived helium and carbon in groundwaters and gases of Mount Etna, Italy. *Earth Planet. Sci. Lett.* 148, 501–516. doi: 10.1016/S0012-821X(97)00052-6
- Amato, A., Azzara, R., Basili, C., Chiarabba, M., Cocco, M., Di Bona, M., et al. (1995). Main shock and aftershocks of the December 13, 1990. *Ann. Geophys.* 38, 255–266. doi: 10.4401/ag-4122
- Arnórsson, S., Gunnlaugsson, E., and Svavarsson, H. (1983). The chemistry of geothermal waters in iceland. iii. chemical geothermometry in geothermal investigations. *Geochim. Cosmochim. Acta* 47, 567–577. doi: 10.1016/0016-7037(83)90278-8
- Asta, M. P., Gimeno, M. J., Auque, L. F., Gomez, J., Acero, P., and Lapuente, P. (2012). Hydrochemistry and geothermometrical modeling of low-temperature Panticosa geothermal system (Spain). *J. Volcanol. Geotherm. Res.* 235, 84–95. doi: 10.1016/j.jvolgeores.2012.05.007
- Aureli, A., Adorni, G., Chiavetta, F., Fazio, F., Fazzina, S., and Messineo, G. (1993). *Carta Della Vulnerabilità Delle Falde Idriche, Settore Nord-Orientale Ibleo (Sicilia SE)*. Florence: University of Catania. doi: 10.1016/j.jvolgeores.2012.05.007
- Barberi, F., Civetta, L., Gasparini, P., Innocenti, F., Scandone, R., and Villari, L. (1974). Evolution of a section of africa-europe plate boundary - paleomagnetic and volcanological evidence from Sicily. *Earth Planet. Sci. Lett.* 22, 123–132. doi: 10.1016/0012-821X(74)90072-7
- Basili, R., Valensise, G., Vannoli, P., Burrato, P., Fracassi, U., Mariano, S., et al. (2008). The database of individual seismogenic sources (DISS), version 3:

## AUTHOR CONTRIBUTIONS

PB and SG conceived the study. GR, PB, and SG did the geothermometric estimates, the statistical analysis, and the PCA analysis of the data. All the authors contributed to the discussion and co-wrote the manuscript.

## SUPPLEMENTARY MATERIAL

The Supplementary Material for this article can be found online at: <https://www.frontiersin.org/articles/10.3389/feart.2019.00088/full#supplementary-material>

- summarizing 20 years of research on Italy's earthquake geology. *Tectonophysics* 453, 20–43. doi: 10.1016/j.tecto.2007.04.014
- Behncke, B. (2004). Late Pliocene volcanic island growth and flood basalt-like lava emplacement in the Hyblean Mountains (SE Sicily). *J. Geophys. Res. Solid Earth* 109:B09201. doi: 10.1029/2003jb002937
- Bertani, R. (2012). Geothermal power generation in the world 2005-2010 update report. *Geothermics* 41, 1–29. doi: 10.1016/j.geothermics.2011.10.001
- Bianchi, F., Carbone, S., Grasso, M., Invernizzi, G., Lentini, F., Longaretti, G., et al. (1987). Sicilia orientale: profilo geologico Nebrodi-Iblei. *Memorie della Società Geologica Italiana* 38, 429–458.
- Blasco, M., Gimeno, M. J., and Auque, L. F. (2018). Low temperature geothermal systems in carbonate-evaporitic rocks: mineral equilibria assumptions and geothermometrical calculations. Insights from the Arnedillo thermal waters (Spain). *Sci. Total Environ.* 615, 526–539. doi: 10.1016/j.scitotenv.2017.09.269
- Bonfanti, P., Carapezza, M. L., D'Alessandro, W., De Domenico, R., Diliberto, I. S., Di Liberto, R., et al. (1993). "Earthquake of december 13, 1990 in eastern Sicily: some geochemical investigations," in *Proceeding of the Scientific Meeting on the Seismic Protection*, (Venice).
- Botteghi, S., Chiesa, S., Destro, E., Di Sipio, E., Galgaro, A., Manzella, A., et al. (2012). *VIGOR: Prime indicazioni tecnico-prescrittive in materia di impianti di climatizzazione geotermica. In Progetto VIGOR - Valutazione del Potenziale Geotermico delle Regioni della Convergenza. POI Energie Rinnovabili e Risparmio Energetico 2007-2013*. Pisa: CNR-IGG.
- Brusca, L., Aiuppa, A., D'Alessandro, W., Parello, F., Allard, P., and Michel, A. (2001). Geochemical mapping of magmatic gas-water-rock interactions in the aquifer of Mount Etna volcano. *J. Volcanol. Geotherm. Res.* 108, 199–218. doi: 10.1016/S0377-0273(00)00286-9
- Carbone, S., Grasso, M., and Lentini, F. (1982). Considerazioni sull'evoluzione geodinamica della Sicilia sud-orientale dal Cretaceo al Quaternario. *Memorie della Società Geologica Italiana* 24, 367–386.
- Carbone, S., Grasso, M., and Lentini, F. (1987). Lineamenti geologici del Plateau Ibleo (Sicilia SE). Presentazione delle carte geologiche della Sicilia sud-orientale. *Memorie della Società Geologica Italiana* 38, 127–135.
- Chiodini, G., Cardellini, C., Amato, A., Boschi, E., Caliro, S., Frondini, F., et al. (2004). Carbon dioxide Earth degassing and seismogenesis in central and southern Italy. *Geophys. Res. Lett.* 31, 2–5. doi: 10.1029/2004gl019480
- Cox, S. F. (1995). Faulting processes at high fluid pressures - an example of fault valve behavior from the Wattle Gully Fault, Victoria, Australia. *J. Geophys. Res. Solid Earth* 100, 12841–12859. doi: 10.1029/95jb00915
- Dall'Aglio, M., Quattrocchi, F., and Tersigni, S. (1995). Geochemical evolution of groundwater of the Iblean Foreland (Southeastern Sicily) after the December 13, 1990 earthquake (M = 5.4). *Ann. Geophys.* 38, 309–329. doi: 10.4401/ag-4126
- D'Amore, F., and Panichi, C. (1985). Geochemistry in geothermal exploration. *Int. J. Energy Res.* 9, 277–298. doi: 10.1002/er.4440090307
- De Gregorio, S., Diliberto, I. S., Giammanco, S., Gurrieri, S., and Valenza, M. (2002). Tectonic control over large-scale diffuse degassing in eastern Sicily (Italy). *Geofluids* 2, 273–284. doi: 10.1046/j.1468-8123.2002.00043.x
- Dolgorjav, O. (2009). Geochemical characterization of thermal fluids from the Khangay area, Central Mongolia. *Geotherm. Train. Programme Rep.* 10, 125–150.



- Fournier, R. O., and Truesdell, A. H. (1973). An empirical Na-K-Ca geothermometer for natural waters. *Geochim. Cosmochim. Acta* 37, 1255–1275. doi: 10.1016/0016-7037(73)90060-4
- Giammanco, S., Ottaviani, M., Valenza, M., Veschetti, E., Principio, E., Giammanco, G., et al. (1998). Major and trace elements geochemistry in the ground waters of a volcanic area: Mount Etna (Sicily, Italy). *Water Res.* 32, 19–30. doi: 10.1016/S0043-1354(97)00198-X
- Giammanco, S., Parello, F., Gambardella, B., Schifano, R., Pizzullo, S., and Galante, G. (2007). Focused and diffuse effluxes of CO<sub>2</sub> from mud volcanoes and mofettes south of Mt. Etna (Italy). *J. Volcanol. Geotherm. Res.* 165, 46–63. doi: 10.1016/j.jvolgeores.2007.04.010
- Giggenbach, W. F. (1988). Geothermal solute equilibria - derivation of Na-K-Mg-Ca geothermometers. *Geochim. Cosmochim. Acta* 52, 2749–2765. doi: 10.1016/0016-7037(88)90143-3
- Grassa, F. (2002). *Geochemical Processes Governing the Chemistry of Groundwater Hosted within the Hyblean Aquifers (Southeastern Sicily, Italy)*. Ph.D. Thesis. Palermo: Univ. of Palermo.
- Grassa, F., Capasso, G., Favara, R., and Inguaggiato, S. (2006). Chemical and isotopic composition of waters and dissolved gases in some thermal springs of Sicily and adjacent volcanic islands, Italy. *Pure Appl. Geophys.* 163, 781–807. doi: 10.1007/s00024-006-0043-0
- Grasso, M., and Lentini, F. (1982). Sedimentary and tectonic evolution of the eastern hyblean plateau (Southeastern Sicily) during late cretaceous to quaternary time. *Palaeogeogr. Palaeoclimatol. Palaeoecol.* 39, 261–280. doi: 10.1016/0031-0182(82)90025-6
- Grasso, M., Lentini, F., and Pedley, H. M. (1982). Late tortonian lower messinian (Miocene) paleogeography of se Sicily - information from 2 new formations of the sortino group. *Sediment. Geol.* 32, 279–300. doi: 10.1016/0037-0738(82)90041-0
- IGA Service GMBH. (2014). *Best Practices Guide for Geothermal Exploration*. Bochum: IGA Service GMBH.
- Labauve, P., Bousquet, J. C., and Lanzafame, G. (1990). Early deformations at a submarine compressive front - the quaternary Catania foredeep south of Mt Etna, Sicily, Italy. *Tectonophysics* 177, 349–366. doi: 10.1016/0040-1951(90)90395-O
- Langelier, W. F., and Ludwig, H. F. (1942). Graphical method for indicating the mineral character of natural waters. *J. Am. Waterworks Assoc.* 34, 335–352. doi: 10.1002/j.1551-8833.1942.tb19682.x
- Lentini, F., Grasso, M., and Carbone, S. (1987). "Introduzione alla geologia della Sicilia e guida all'escursione," in *Proceedings of the Convegno Soc. Geol. It. "Sistemi Avanfoss-Avampaese Lungo la Catena Appenninico-Maghrebide."*, (Naxos-Pergusa).
- Minissale, A., Donato, A., Procesi, M., Pizzino, L., and Giammanco, S. (2019). Systematic review of geochemical data from thermal springs, gas vents and fumaroles of Southern Italy for geothermal favourability mapping. *Earth Sci. Rev.* 188, 514–535. doi: 10.1016/j.earscirev.2018.09.008
- Morales-Arredondo, J. I., Esteller-Alberich, M. V., Hernandez, M. A. A., and Martinez-Florentino, T. A. K. (2018). Characterizing the hydrogeochemistry of two low-temperature thermal systems in Central Mexico. *J. Geochem. Explorat.* 185, 93–104. doi: 10.1016/j.gexplo.2017.11.006
- Nicholson, K. (1993). *Geothermal Fluids. Chemistry and Exploration Techniques*. Berlin: Springer. doi: 10.1016/j.gexplo.2017.11.006
- Rice, J. R. (1992). "Fault stress states, pore pressure distributions, and the weakness of the San Andreas fault," in *Fault Mechanics and Transport Properties of Rocks: A Festschrift in Honor of*, eds B. Evans, cpsfmT.-f. cpefmWong, and W. F. Brace (San Diego: Academic Press), 476–503.
- Ristuccia, G. M., Di Stefano, A., Gueli, A. M., Monaco, C., Stella, G., and Troja, S. O. (2013). OSL chronology of quaternary terraced deposits outcropping between Mt. Etna volcano and the Catania Plain (Sicily, southern Italy). *Phys. Chem. Earth* 63, 36–46. doi: 10.1016/j.pce.2013.03.002
- Ruggieri, R. (1990). "Assetto idrogeologico e intrusione delle acque marine nell'entroterra costiero ibleo," in *Proceedings of the 1st Convegno Nazionale di Idrogeologia*, (Modena).
- Sanliyüksel, D., and Baba, A. (2011). Hydrogeochemical and isotopic composition of a low-temperature geothermal source in northwest Turkey: case study of Kirkgöçit geothermal area. *Environ. Earth Sci.* 62, 529–540. doi: 10.1007/s12665-010-0545-z
- Schiano, P., Clocchatti, R., Ottolini, L., and Busá, T. (2001). Transition of Mount Etna lavas from a mantle-plume to an island-arc magmatic source. *Nature* 412, 900–903.
- Schmincke, H.-U., Behncke, B., Grasso, M., and Raffi, S. (1997). Evolution of the northwestern Iblean Mountains, Sicily: uplift, pliocene/pleistocene sea-level changes, paleoenvironment, and volcanism. *Geol. Rundsch.* 86, 637–669. doi: 10.1007/s005310050169
- Sibson, R. H. (1992). Fault-valve behavior and the hydrostatic lithostatic fluid pressure interface. *Earth Sci. Rev.* 32, 141–144. doi: 10.1016/0012-8252(92)90019-P
- Sibson, R. H. (2000). Fluid involvement in normal faulting. *J. Geodyn.* 29, 469–499. doi: 10.1016/S0264-3707(99)00042-3
- Sortino, F., Inguaggiato, S., and Francofonte, S. (1991). Determination of HF, HCl, and total sulfur in fumarolic fluids by ion chromatography. *Acta Vulcanol.* 1, 89–91.
- Swan, A. R. H., and Sandilands, M. H. (1995). *Introduction to Geological Data Analysis*. Hoboken, NJ: Blackwell Science Ltd.
- Zervos, A., Lins, C., and Tesnière, L. (2011). *Mapping Renewable Energy Pathways towards 2020 - EU Roadmap*. Bruxelles: European Renewable Energy Council.

**Conflict of Interest Statement:** The authors declare that the research was conducted in the absence of any commercial or financial relationships that could be construed as a potential conflict of interest.

Copyright © 2019 Ristuccia, Bonfanti, Giammanco and Stella. This is an open-access article distributed under the terms of the Creative Commons Attribution License (CC BY). The use, distribution or reproduction in other forums is permitted, provided the original author(s) and the copyright owner(s) are credited and that the original publication in this journal is cited, in accordance with accepted academic practice. No use, distribution or reproduction is permitted which does not comply with these terms.